https://doi.org/10.3311/PPci.19894

Periodica Polytechnica Civil Engineering, 66(3), pp. 843–852, 2022

Simple Equations for Predicting Maximum Displacement of Isolation Systems Using Lead Rubber Bearings

Nhan Dinh Dao[1*]

[1] Faculty of Civil Engineering, University of Architecture Ho Chi Minh City, 196 Pasteur, Ward 6, District 3, Viet Nam
[*] Corresponding author, e-mail: nhan.daodinh@uah.edu.vn

Received: 23 January 2022, Accepted: 05 April 2022, Published online: 12 May 2022

Abstract

Predicting maximum displacement is an important task in designing isolation systems. An effective procedure that is widely used for this task is equivalent linear force (ELF) procedure, which is allowed by many contemporary design codes. This procedure uses very basic parameters of the isolation system as well as earthquake condition of the site to analyze for the maximum displacement. However, ELF procedures are time-consuming because they require an iteration process. This study employed an ELF procedure to generate a large database and used it to develop explicit and simple equations that can directly calculate the maximum displacement of isolation systems using lead rubber bearings. The proposed equations can confidently predict the maximum displacement calculated by the ELF procedure. In addition, the investigation showed that the first to post-yield stiffness ratio of an isolation system, which is difficult to accurately determine, has neglected effect on the maximum displacement calculated by the ELF procedure. Based on this observation, a simple equation that uses only three input parameters to predict the maximum displacement was proposed. The input parameters to the simplified equation include normalized characteristic strength and post-yield period of the isolation system, and 1-s spectral acceleration of the site. These parameters are minimum to determine an isolation system and earthquake condition. The comparison between the maximum displacement predicted by the proposed equation and the maximum displacement calculated by the ELF procedure showed that the proposed equation generates slightly conservative results for common designs, therefore is suitable for practical application.

Keywords

lead rubber bearing, maximum displacement, equivalent linear force procedure, isolation system, earthquake response

1 Introduction

Lead rubber bearings (LRBs) can effectively protect buildings during earthquakes by isolating them from the ground, thus limiting the seismic energy transferred to the isolated buildings. A typical LRB (demonstrated in Fig. 1) consists of alternative layers of steel and rubber surrounding a lead core. These components are mounted between two thick steel plates which are connected to the column base of the building and the foundation. This composition provides the bearing rigidity in the vertical direction and flexibility in the horizontal direction. The rigidity and strength in the vertical direction help the bearing to support the weight of the isolated building while the horizontal flexibility lengthens the fundamental period of the isolated building, therefore reduces the base shear exerting to the superstructure. The lead core in the bearing helps resisting small horizontal load caused by small earthquakes and wind without significant deformation. Its hysteresis behavior during strong earthquakes dissipates seismic energy transferred to the superstructure.

The flexibility of LRBs renders the isolated building safer during earthquakes. Meanwhile, it also introduces large relative displacement between the isolated building

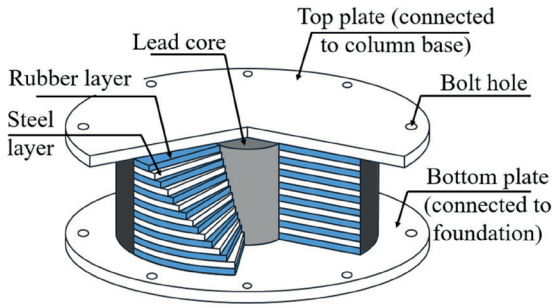

Fig. 1 Composition of an LRB

Cite this article as: Dao, N. D. "Simple Equations for Predicting Maximum Displacement of Isolation Systems Using Lead Rubber Bearings", Periodica Polytechnica Civil Engineering, 66(3), pp. 843–852, 2022. https://doi.org/10.3311/PPci.19894

and the ground. This may cause collision between the isolated building and surrounding structures if insufficient isolation gap is provided. The large deformation in the bearings subjected to the large relative displacement can also damage the isolation system. Accurately predicting maximum displacement of the isolation system during earthquakes, therefore, is critical to design for these circumstances.

Time-history dynamic analysis of the nonlinear model is the most rigorous approach to predict maximum displacement of an isolation system. However, this approach is time-consuming and complicated due to many issues. Firstly, this approach requires time-history input of ground motions, whose availability is limited to most area in the world. Selecting, scaling, or simulating ground motions for a site demands some extensive level of expertise. Secondly, constructing and analyzing the nonlinear model of the system expect solid knowledge in the field. Furthermore, validation and interpretation of the analysis results also request experienced analysts. These difficulties intimidate the application of time-history analysis procedure.

To overcome the difficulty of time-history analysis procedure, contemporary design codes such as ASCE 7-16 [1] and EN-1998 [2] allow equivalent linear force (ELF) procedures, which are much simpler than time-history analysis procedure, to be used to estimate the maximum displacement of an isolation system, providing that it satisfies some specific conditions. In practice, ELF procedures are usually applied during the preliminary design phase of any isolation system.

The most-used ELF procedure is rooted in the secant stiffness at steady state harmonic amplitude proposed by Rosenblueth and Herrera [3] and the equivalent viscous damping model proposed by Jacobsen [4]. According to Rosenblueth and Herrera [3], the steady amplitude of a slightly nonlinear material model is similar to that of a linear viscoelastic model whose stiffness equals the secant stiffness at the peak displacement of the nonlinear model and damping is determined such that the dissipated energy in one cycle of the two models are the same, i.e., following Jacobsen [4] approach. The linear viscoelastic model whose stiffness and damping are determined from this approach is hereafter referred to as 'equivalent linear model'. Extending this result to the response to earthquake inputs, the maximum displacement of a slightly nonlinear model subjected to an earthquake ground motion can be estimated based on its equivalent linear model.

Since the maximum displacement of a linear model subjected to an earthquake ground motion can be determined from its response spectra, the design maximum displacement can be determined from design spectra without having to perform time-history analysis. This advantage makes the ELF procedure attractive to practical engineers.

However, it is worth noting that earthquake inputs are not harmonic, therefore the maximum displacement calculated from the ELF procedure may not equal the maximum displacement determined from time-history analysis procedure. Some researchers have investigated the accuracy of the ELF procedure and concluded that it yields reasonable results [5–11], especially when some modifications are applied [12]. Contrarily, some studies showed that the procedure is either un-conservative or inefficient [13–18]. Nevertheless, the procedure is allowed in modern design codes [1, 2] and is widely used due to its simplicity.

Although the ELF procedure is simple, it requires iteration (see Section 3) thus is time-consuming. This study developed explicit equations that predict the maximum displacement of isolation systems using lead rubber bearings subjected to earthquakes without iterating. These practical equations use minimum number of input parameters and aim to generate results that match the results computed from the ELF procedure.

2 Idealized bi-linear behavior of isolation systems

Unidirectional behavior in a horizontal direction of an LRB can be idealized by a kinematic strain-hardening bilinear hysteretic model as shown in Fig. 2 [19]. The constitutive parameters that control the loop include characteristic strength F_d, post yield stiffness K_d and initial stiffness K_1. Other important parameters such as yield displacement D_y and yield strength F_y can be easily calculated from the three constitutive parameters. For an LRB, F_d can be calculated from the yield stress and the area of its lead core (mind the difference between yield load level F_d of the core and F_y of the entire bearing); K_d is estimated from the shear modulus of rubber and bearing design

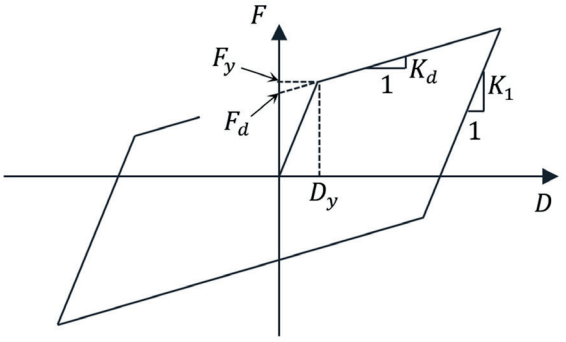

Fig. 2 Bilinear behavior of isolation bearings

(i.e., the size, the shape, and the number of rubber layers of the bearing); K_1 is difficult to determine and is usually assumed as a factor of K_d [19, 20], or assumed through a yield displacement D_y [21, 22].

For an isolation system composed of many bearings in parallel, the behavior of the system can be derived by adding the behavior of all the bearings. Specifically, the constitutive parameters K_1, F_d and K_d of all bearings in the system shall be added up. Therefore, the bilinear model shown in Fig. 2 can also be used to represent the behavior of an isolation system.

Two other important engineering parameters of an isolation system are effective stiffness K_M and effective damping ratio β_M at maximum displacement D_M. For the bilinear behavior demonstrated in Fig. 2, these two engineering parameters can be computed by [19]:

$$K_M = K_d + F_d / D_M , \tag{1}$$

$$\beta_M = \frac{2F_d\left(D_M - D_y\right)}{\pi\left(K_d.D_M + F_d\right)D_M} , \tag{2}$$

where D_y is computed from F_d, K_1 and K_d as follows:

$$D_y = F_d / \left(K_1 - K_d\right). \tag{3}$$

Effective period T_M of the system correspondent to effective stiffness can be computed by:

$$T_M = 2\pi\sqrt{W / gK_M} , \tag{4}$$

where W is the weight of the isolated building.

For convenience, the behavior and engineering parameters of an isolation system are normalized by W. They are also expressed in terms of the post-yield period T_d, normalized characteristic strength f_d, and initial to post-yield stiffness ratio k_{1d} of the isolation system defined by Eqs. (5)–(7).

$$T_d = 2\pi\sqrt{W / gK_d} \tag{5}$$

$$f_d = F_d / W \tag{6}$$

$$k_{1d} = K_1 / K_d \tag{7}$$

Equations (5)–(7) can be rewritten as:

$$K_d = 4\pi^2 W / gT_d^2 \tag{8}$$

$$F_d = f_d W \tag{9}$$

$$K_1 = k_{1d} K_d \tag{10}$$

Substituting Eqs. (8)–(10) into Eq. (3) yields:

$$D_y = gT_d^2 f_d / 4\pi^2\left(k_{1d} - 1\right). \tag{11}$$

Substituting Eqs. (8-9) into Eq. (2) yields:

$$\beta_M = 2gT_d^2 f_d\left(D_M - D_y\right) / \pi\left(4\pi^2 D_M + gT_d^2 f_d\right)D_M . \tag{12}$$

Substituting Eqs. (8–9) into Eq. (1) for K_M then substituting to Eq. (4) yields:

$$T_M = 2\pi\sqrt{1/\left(4\pi^2 / T_d^2 + gf_d / D_M\right)} . \tag{13}$$

Eqs. (11–13) show that effective period T_M and effective damping ratio β_M at a maximum displacement D_M are dependent on f_d, T_d, and k_{1d}.

3 Equivalent linear force procedure

Many contemporary design codes allow using ELF procedures to predict the maximum displacement of an isolation system, providing that specific requirements are satisfied. This study employed the ELF procedure in ASCE 7-16 [1] to generate the data for constructing simple equations. The requirement for applying ELF procedure according to this code is summarized as following:

1. The site class in consideration is either A, B, C or D.
2. The effective period of the system at the maximum displacement D_M (determined at risk-targeted maximum considered earthquake, MCER, level) must not exceed 5.0 s.
3. The height of the superstructure does not exceed 19.8 m, or no tension or uplift on the isolators occurs.
4. The effective damping ratio of the isolation system at D_M does not exceed 0.3.
5. The effective period of the system at D_M is greater than three times of the period of the fixed-base superstructure.
6. The superstructure is not irregular.
7. The isolation system meets these criteria: (a) the effective stiffness at D_M is greater than one third of the effective stiffness at 0.2 D_M, (b) the restoring force at D_M is at least 0.025 W greater than the restoring force at 0.5 D_M, where W is the weight of the superstructure, and (c) the isolation system does not limit the displacement to less than the total displacement D_{TM} which is the maximum displacement accounting for the torsion displacement due to the mass eccentricity of the isolated structure.

The ELF procedure neglects the flexibility and damping of superstructure and considers the whole system

as a linear single degree of freedom (SDF) system. The natural period and damping ratio of the linear SDF system equal the effective period T_M and effective damping ratio β_M, respectively, of the isolation system. For a linear SDF system, the maximum displacement D_M correspondent to T_M and β_M can be calculated by [23]:

$$D_M = T_M^2 A_M / 4\pi^2, \tag{14}$$

where A_M is the spectral acceleration correspondent to natural period T_M and damping ratio β_M.

ASCE 7-16 [1] allows A_M to be calculated from 5%-damped spectral acceleration A at natural period T_M as shown in Eq. (15):

$$A_M = A / B_M, \tag{15}$$

where B_M is a damping correction factor to convert the 5%-damped spectral acceleration A to the spectral acceleration A_M at damping ratio β_M. The value of B_M at different β_M can be looked up from Table 1 [1].

For simplicity, assume that the effective period T_M of the isolation system in consideration falls into the constant-velocity region of the elastic design spectrum, then the 5%-damped spectral acceleration A at T_M can be computed from the 5%-damped spectral acceleration A_1 at 1-s period as follows:

$$A = A_1 / T_M. \tag{16}$$

Combining Eqs. (14)–(16) yields:

$$D_M = T_M A_1 / 4\pi^2 B_M. \tag{17}$$

Equation (17) indicates that for a certain 1-s spectral acceleration A_1 (at 5%-damped), the maximum displacement D_M of an isolation system can be calculated from its effective period T_M and effective damping ratio β_M (which affects B_M), which in turn are dependent on D_M as shown in Eqs. (12)–(13). This means that D_M can only be determined through an iteration process. An iteration procedure for solving D_M is presented in the following steps:

Table 1 Damping correction factor at different damping ratio

Damping ratio β_M	Damping correction factor B_M
≤ 0.02	0.8
0.05	1.0
0.1	1.2
0.2	1.5
0.3	1.7
0.4	1.9
≥ 0.5	2.0

B_M shall be based on linear interpolation for β_M other than those given on the table.

Step 1: Assume an arbitrary value of D_M.

Step 2: Compute T_M and β_M from Eqs. (11)–(13).

Step 3: Look up for B_M from Table 1.

Step 4: Compute D_M from Eq. (17).

Step 5: Repeat Steps 2 to 4 until D_M converges.

An example demonstrating this procedure is presented in Section 6.

4 Data generation

This study employed a regression approach to develop simple equations for predicting the maximum displacement of an isolation system. The database for this process was generated following the ELF procedure described in Section 3. Recall that the maximum displacement of an isolation system computed from the ELF procedure is dependent on normalized characteristic strength f_d, post-yield period T_d, first to post-yield stiffness ratio k_{1d}, and 1-s spectral acceleration A_1. To generate the database that covers most practical applications, wide ranges of the input parameters were considered. These ranges are listed in Table 2. The ranges of isolation system parameters were selected to cover recommended values from practice guidelines as well as past studies. Specifically, the design guideline from Holmes Consulting Group [20] suggested that f_d usually ranges from 0.03 (at low seismic zones) to 0.1 (at high seismic zones). Park and Otsuka [24] mentioned that the design procedure from Dynamic Isolation System Inc. (DIS) uses f_d = 0.03 to 0.07. In that study, they also proposed optimal values of f_d, which ranges from 0.02 to 0.14, as a function of peak ground acceleration. For the purpose of evaluating an equivalent lateral force procedure, Ozdemir and Constantinou [11] investigated isolation systems with f_d ranges from 0.04 to 0.14 and T_d ranges from 3.0 s to 4.5 s. A Similar study by Pant et al. [22] investigated isolation systems with f_d = 0.03 to 0.09 and T_d = 2.5 s to 5.5 s. Mavronicola and Komodromos [25], Liu et al. [26] also used isolation systems with f_d falling into this range (e.g., f_d = 0.1 and 0.05, respectively) in their studies. Naeim and Kelly [19] commented that the effective period T_{eff} of an isolation system is expected to fall between 2.0 s to 3.0 s. This range also agrees with the recommendation from a document of DIS [27]. To produce

Table 2 Input parameters

Parameter	Minimum value	Maximum value	Increment
f_d	0.02	0.16	0.01
T_d (s)	2.0	6.0	0.5
k_{1d}	5	25	5
A_1 (g)	0.4	1.2	0.1

this T_{eff}, T_d must be larger than 2.0 s. In an introduction to base isolation design practice in Japan, Pan et al. [28] advised that T_d should be larger than 3.5 s. The k_{1d} range, which spans from 5 to 25, has been widely opted [19, 20, 24–26]. Some other studies [11, 22] did not use k_{1d}. Instead, they set a fixed yield displacement for the isolation systems. This discrepancy occured because k_{1d} of an LRB isolation system is difficult to be accurately determined. Luckily, this ratio has little effect on the accuracy of the proposed equations in this study, as shown later.

The A_1 range listed in Table 2 is considered to be suitable for high seismic zones, where seismic isolation technique is appreciated. Most of the mentioned studies [11, 19, 20, 22, 25, 26] investigated A_1 or PGA well below 1.2 g, except the study of Park and Otsuka [24], which investigated PGA up to 1.225 g. The lower bound of PGA in some of these studies were slightly lower than 0.4 g. However, as presented next, the participation of small A_1 in the accepted samples is insignificant. These imply that the considered range of A_1 covers most practical applications.

The combination of the isolation system parameters listed in Table 2 results in 675 isolation systems. These isolation systems subjected to nine values of A_1 yields 6,075 cases to analyze for the maximum displacement D_M. Only isolation systems and maximum displacements that satisfy the requirement of the ELF procedure described in Section 3 were accepted for processing. Accordingly, a total number of 3,028 samples was opted.

Fig. 3 shows frequency distribution and cumulative distribution of the maximum displacement D_M. The minimum value, maximum value and mean value of D_M in the selected database are 0.081 m, 1.433 m and 0.479 m, respectively. 86.3% of D_M fall between 0.1 m to 0.75 m.

Frequency distribution of input parameters in the selected samples are shown in Fig. 4. It is observed that these distributions are not uniform, although their seeds were generated from uniform distributions. This comes from the fact that only samples that satisfy the ELF procedure requirement were selected. Large value of A_1, small value of f_d and T_d possess high opportunity to appear in the selected database.

5 Developing simple equations

As shown in Section 3, four parameters influencing the maximum displacement D_M of an isolation system computed from the ELF procedure include 1-s spectral acceleration A_1, post-yield period T_d, normalized characteristic strength f_d, and first to post-yield stiffness ratio k_{1d}.

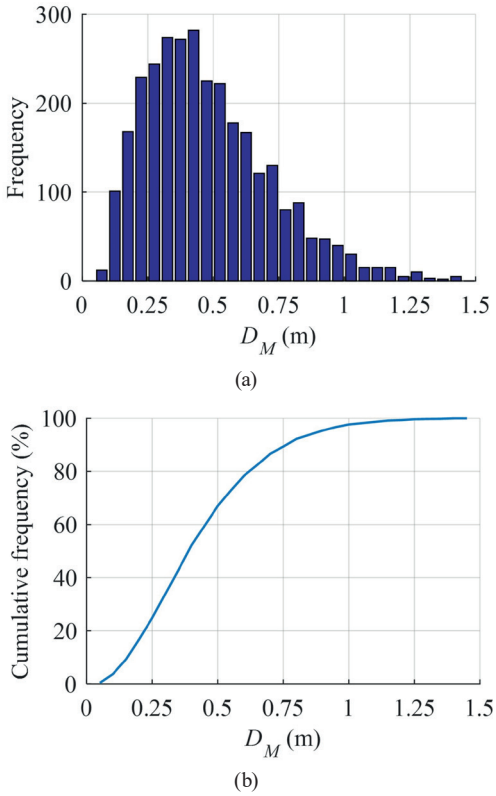

Fig. 3 Distribution of maximum displacement D_M: a) Frequency distribution; b) Cumulative distribution

To construct simple equations, this study assumes that the maximum displacement can be approximated by $\bar{D}_M$ which is a function of the four influencing parameters as following:

$$\bar{D}_M = a \times A_1^b \times T_d^c \times f_d^d \times k_{1d}^e , \tag{18}$$

where a, b, c, d and e are coefficient and powers to be determined so that this function can confidently predict the maximum displacement in the generated database.

To derive the coefficient and powers in Eq. (18), a nonlinear regression tool was applied to minimize the error function defined by Eq. (19).

$$\varepsilon = \sum_{i=1}^{N} \left(\frac{\bar{D}_{Mi} - D_{Mi}}{D_{Mi}} \right)^2 , \tag{19}$$

where N = 3,028 is the total number of samples in the selected database; D_{Mi} is the maximum displacement of sample i, which was computed from the ELF procedure; and $\bar{D}_{Mi}$ is the approximate displacement computed from the input parameters in sample i following Eq. (18).

According to the Sequential Least Squares Programming optimizer from "scipy" Python library [29] the value of coefficient and powers that minimize ε are a = 0.002590, b = 1.4838, c = 0.5113, d = –0.4929, and e = –0.03006.

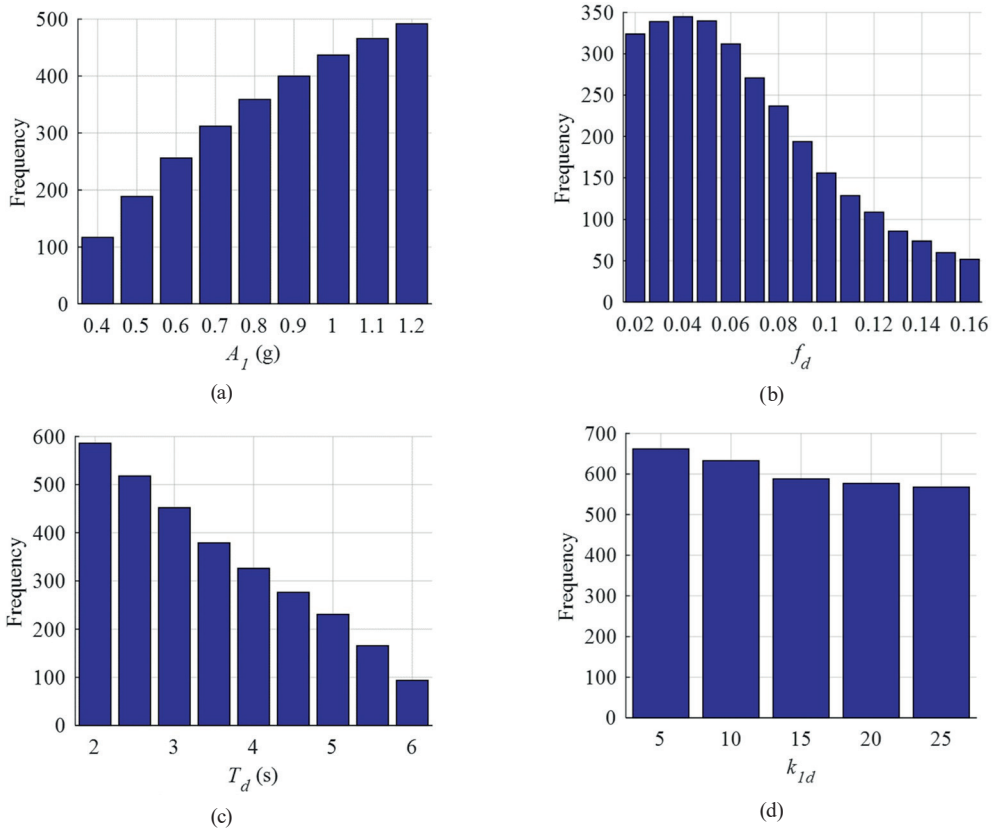

Fig. 4 Distribution of input parameters: a) Distribution of A_1; b) Distribution of f_d; c) Distribution of T_d; d) Distribution of k_{1d}

Therefore, Eq. (18) can be rewritten as:

$$\bar{D}_M = 0.00259 \times \frac{A_1^{1.4838} \times T_d^{0.5113}}{f_d^{0.4929} \times k_{1d}^{0.03006}}. \quad (20)$$

Note that $\bar{D}_M$, A_1 and T_d in this equation are measured in m, m/s² and s, respectively; f_d and k_{1d} are unitless.

In practice, 1-s spectral acceleration is usually expressed in term of g, where g = 9.81 m/s² is gravity acceleration. Let:

$$S_1 = A_1 / g. \quad (21)$$

Equation (20) becomes:

$$\bar{D}_M = 0.0767 \times \frac{S_1^{1.4838} \times T_d^{0.5113}}{f_d^{0.4929} \times k_{1d}^{0.03006}}. \quad (22)$$

Fig. 5 plots the maximum displacements $\bar{D}_M$ predicted by Eq. (22) against the maximum displacements D_M calculated by the ELF procedure for all selected samples. The fitted line representing the relationship between $\bar{D}_M$ and D_M is also shown in the figure. The equation of the fitted line is:

$$\bar{D}_M = 0.9995 D_M - 0.0005. \quad (23)$$

The coefficient of determination of the relationship is R^2 = 0.9934. These results show that Eq. (22) well predicts the maximum displacement calculated by the ELF procedure.

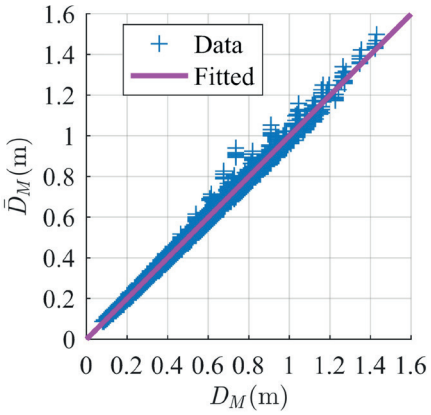

Fig. 5 $\bar{D}_M$ predicted by Eq. (22) vs D_M

It is noted that the power of k_{1d} in Eq. (22), as well as Eq. (20), is small. In the investigated data where k_{1d} ranges from 5 to 25, $k_{1d}^{0.03006}$ varies from 1.0496 to 1.1016, which changes around 5%. This implies that k_{1d} has small effect on $\bar{D}_M$. Taking a closer look at the selected database confirms that k_{1d} has small effect on D_M. For example, Fig. 6 shows the effect of k_{1d} on D_M of 100 random data sets. To construct this graph, 100 data sets were randomly selected from the investigated database. Each data set contains all samples having the same value of S_1, T_d, and f_d but different value of k_{1d}. This means that the variation of D_{Mv} in one data set comes solely from the variation of k_{1d} between the samples.

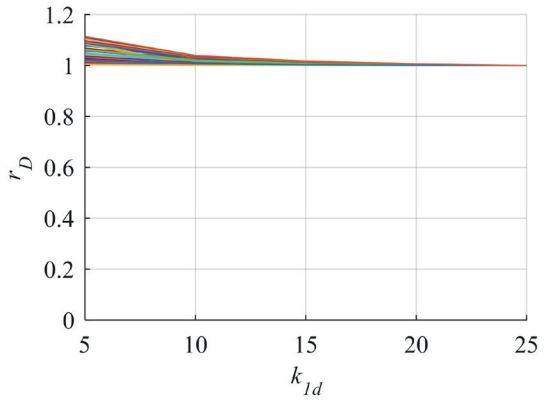

Fig. 6 Effect of k_{1d} on maximum displacement

The horizontal axis of the graph represents k_{1d} while the vertical axis represents the displacement ratio r_D which was computed by dividing D_M at the correspondent k_{1d} by D_M at largest k_{1d} in the set (which was usually 25). Each line in the graph represents one data set among the 100 randomly selected sets. The result from this figure shows that r_D does not change significantly in the investigated range of k_{1d}, which means that has small effect on D_M.

Since has insignificant effect on $\bar{D}_M$ and it is difficult to determine as mentioned before, a regression function for predicting $\bar{D}_M$ without k_{1d} was constructed and is shown in Eq. (24).

$$\bar{D}_M = 0.07117 \times \frac{S_1^{1.4824} \times T_d^{0.5127}}{f_d^{0.4915}} \tag{24}$$

The relationship between D_M and $\bar{D}_M$ calculated by Eq. (24) for all selected samples is plotted in Fig. 7. The fitted line, whose equation is shown in Eq. (25), is also plotted. Coefficient of determination of the relationship is $R^2 = 0.9928$, which is slightly lower than the R^2 of the relationship in Fig. 5.

$$\bar{D}_M = 0.9977 D_M - 0.00004 \tag{25}$$

For practical application, Eq. (24) can be simplified to:

$$\bar{D}_M = 0.07 S_1^{1.5} T_d^{0.5} / f_d^{0.5} = 0.07 \sqrt{S_1^3 T_d / f_d} \,. \tag{26}$$

Fig. 8 shows the relationship between D_M and $\bar{D}_M$ calculated from Eq. (26) throughout the investigated database. The equation of the best fit line of this relationship is:

$$\bar{D}_M = 0.9959 D_M - 0.0031 \,. \tag{27}$$

The coefficient of determination for this relationship is $R^2 = 0.992$.

To investigate the conservativeness of $\bar{D}_M$ predicted by Eq. (26), the displacement ratio r defined by Eq. (28) was computed for all samples in the investigated database. Note that $\bar{D}_M$ in this equation was computed per Eq. (26).

$$r = \bar{D}_M / D_M \tag{28}$$

Fig. 9 plots the value of r against their correspondent for all investigated samples. The value of r accumulates around unit as expected. Minimum and maximum values of r are respectively 0.933 and 1.251. A closely looking at the data revealed that the outliers where r is significantly lager than others came from the isolation systems having very low f_d and T_d subjected to very high S_1. Specifically, all

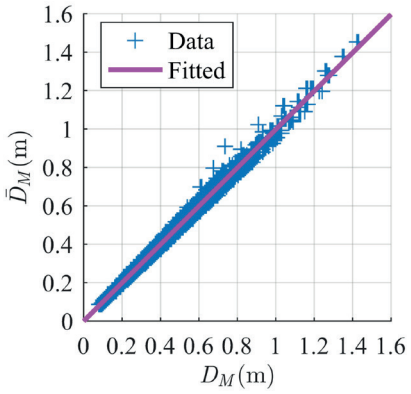

Fig. 7 $\bar{D}_M$ predicted by Eq. (24) vs. D_M

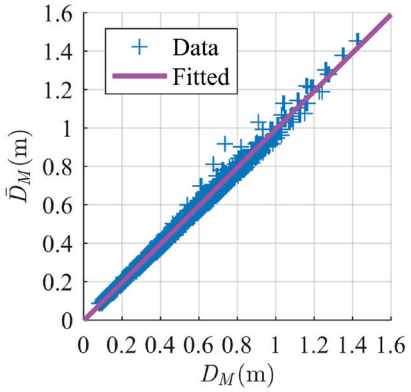

Fig. 8 $\bar{D}_M$ predicted by Eq. (26) vs. D_M

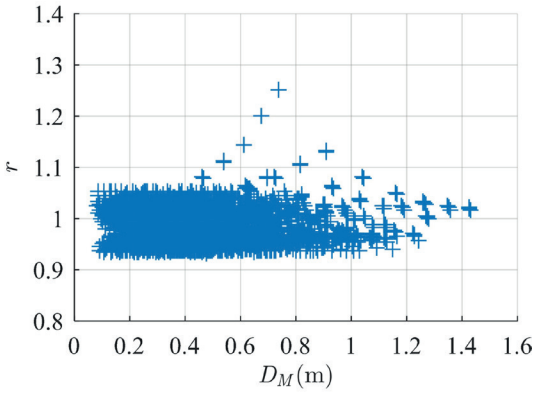

Fig. 9 $\bar{D}_M$ predicted by Eq. (26) vs. D_M

cases where $r \geq 1.1$ came from the isolation systems having $f_d = 0.0.2$ and $T_d \leq 2.5$ subjected to $S_1 \geq 0.9$ to produce D_M larger than 0.5 m. These cases produced very small effective damping ratio β_M (i.e., smaller than 0.025) at maximum displacement, therefore is unrealistic because ones would not design isolation system with this very low β_M.

The relationship between r and β_M over all samples are presented in Fig. 10. The graph confirms that very high r are correspondent to very low β_M. This result means that Eq. (26) does not significantly overestimate D_M for usual applications.

Recall that the smallest value of r was 0.933. Thus, a conservative equation that does not produce $\bar{D}_M$ smaller than D_M can be derived by dividing the right hand side of Eq. (26) by 0.933. As the result, Eq. (29) was yielded.

$$\bar{D}_M = 0.075\sqrt{S_1^3 T_d / f_d} \tag{29}$$

The maximum displacement predicted by this equation is 7.1% larger than that predicted by Eq. (26).

Fig. 11 shows the relationship between D_M and $\bar{D}_M$ computed from Eq. (29) for all investigated samples. The data points accept the line $\bar{D}_M = D_M$ as the lower bound. The minimum ratio of $\bar{D}_M / D_M$ over all data points is 1.000.

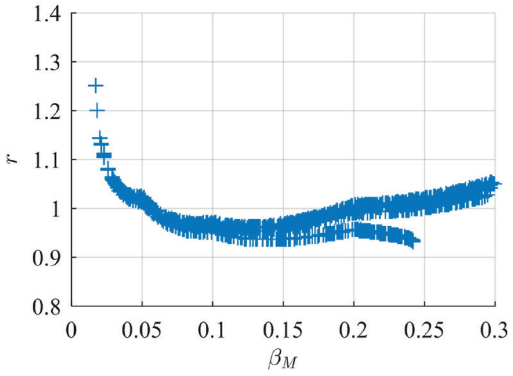

Fig. 10 r vs. β_M

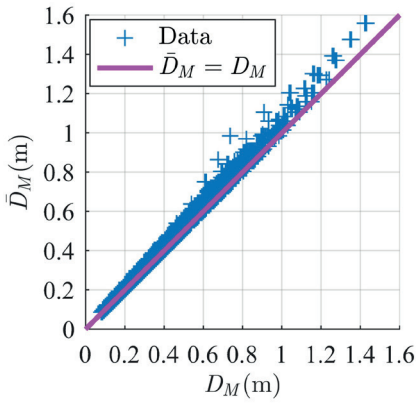

Fig. 11 D_M vs. $\bar{D}_M$ computed from Eq. (29)

These results confirm that Eq. (29) can be used to calculate the lower bound of maximum displacement predicted by the ELF procedure for the investigated database, which expects to cover most practical designs.

Refer to Fig. 10, in the range where $0.1 \leq \beta_M \leq 0.2$, which is common in practice [20], the displacement ratio r can be very low. Therefore, Eq. (29) should be used in practice for conservative.

6 Example

This example employed the benchmark isolation system designed by Naeim and Kelly [19] to demonstrate the application of the proposed equations. The properties of the isolation system are listed in Table 3.

The 1-s spectral acceleration for the maximum considered earthquake level of the site is $A_1 = 0.7$ g (i.e., $S_1 = 0.7$).

6.1 Calculate maximum displacement using the ELF procedure

Apply iteration procedure in Section 3 to calculate for maximum displacement D_M.

For the first iteration, assume $D_M = 0.5$ m.

From Eqs. (12)–(13): $\beta_M = 0.10082$, $T_M = 2.761$ s.

Look up for B_M from Table 1: $B_M = 1.2025$.

Re-calculate D_M using Eq. (17): $D_M = 0.3994$ m.

Use this new D_M, re-calculate β_M, T_M, B_M, then update D_M and repeat the calculation until the result converges. Table 4 shows the result for the first six iterations. The numbers are reported with 4 significant digits, except for the numbers beginning with 1, which possesses 5 significant digits.

According to Table 4, the accuracy in the order of cm stops the iterating process after four iterations, the accuracy in the order of mm requires six iterations. The initial guess $D_M = 0.3$ m also requires the same number of iterations to yield these accuracies.

Table 3 Properties of the isolation system designed by Naeim and Kelly

Property	Unit	Value
Building weight, W	N	16×10^6
Post-yield stiffness, K_d	N/m	7.08×10^6
Characteristic strength, F_d	N	0.684×10^6
Yield displacement, D_y	m	0.011
Normalized characteristic strength, f_d	-	0.04275
Initial stiffness, K_1	N/m	69.26×10^6
Stiffness ratio, k_{1d}	-	9.782
Post-yield period, T_d	s	3.016

Table 4 Iteration for calculating D_M (Example 1)

Iteration	Trial D_M (m)	β_M	T_M (s)	B_M	D_M (m)
1	0.5	0.10082	2.761	1.2025	0.3994
2	0.3994	0.12059	2.706	1.2618	0.3731
3	0.3731	0.12709	2.688	1.2813	0.3649
4	0.3649	0.12926	2.682	1.2878	0.3622
5	0.3622	0.12998	2.68	1.2899	0.3613
6	0.3613	0.13022	2.679	1.2907	0.3610

6.2 Calculate maximum displacement using the proposed practical equations

Instead of using the iteration process, the maximum displacement can be estimated by the proposed practical equations. Specifically, according to Eq. (29), $\bar{D}_M = 0.3689$ m. In the order of mm, this result, i.e., 0.369 m, is 2.22% larger than the result obtained from iteration process. The results calculated from Eqs. (22) and (26) are respectively 0.351 m and 0.344 m, which are lower than the result from the iteration process by 2.77% and 4.7%, respectively.

These results certify that Eq. (29) slightly conservatively estimates the maximum displacement computed from the ELF procedure.

7 Conclusions

This study developed simple equations for predicting maximum displacement of isolation systems using lead rubber bearings. The database for regressing these equations was generated following the equivalent linear force (ELF) procedure described in ASCE 7-16 [1]. The primary equation (i.e., Eq. (22)) uses four inputs to predict the maximum displacement. These inputs include three parameters describing the isolation system, which are normalized characteristic strength f_d, post-yield period T_d and first to post-yield stiffness ratio k_{1d}, and one parameter representing earthquake condition of the site, which is 1-s spectral acceleration coefficient S_1. The coefficient and powers of the proposed equation were selected to minimize the discrepancy between the predicted maximum displacement and the maximum displacement computed from the ELF procedure.

A detail investigation indicated that k_{1d} has insignificant effect on the predicted maximum displacement. Therefore, an equation which is independent on k_{1d} was constructed (Eq. (24)). The advantage of this equation is that it does not require k_{1d}, which is very difficult to determine, to calculate the maximum displacement. An approximate form, which uses simpler coefficient and powers, of Eq. (24) was also proposed and is presented in Eq. (26).

All the above equations, i.e., Eqs. (22), (24) and (26), may result in un-conservative prediction for usual isolation systems. Therefore, a simple and conservative, but not overly conservative for most actual applications, equation was proposed as shown in Eq. (29). This equation should be used in practice.

The proposed equations were derived from the investigation of isolation systems with $f_d = 0.02$ to 0.16, $T_d = 2.0$ s to 6.0 s, $k_{1d} = 5$ to 25 subjected to $S_1 = 0.4$ to 1.2.

References

[1] ASCE "ASCE/SEI 7-16 Minimum design loads and associated criteria for buildings and other structures", American Society of Civil Engineers, Reston, VA, USA, 2017. https://doi.org/10.1061/9780784414248

[2] CEN "EN 1998-1, Eurocode 8: Design of structures for earthquake resistance", European Committee for Standardization, Brussels, Belgium, 2004.

[3] Rosenblueth, E., Herrera, I. "On a Kind of Hysteretic Damping", Journal of Engineering Mechanics Division, 90(4), pp. 37–48, 1964. https://doi.org/10.1061/JMCEA3.0000510

[4] Jacobsen, L. S. "Damping in composite structures", Proceedings of the Second World Conference on Earthquake Engineering, 2, pp. 1029–1044, 1960.

[5] Theodossiou, D., Constantinou, M. C. "Evaluation of SEAOC design requirements for sliding isolated structures", University of Buffalo (SUNY), Buffalo, NY, USA, Rep. NCEER-91-0015, 1991.

[6] Hwang, J. S. "Evaluation of Equivalent Linear Analysis Methods of Bridge Isolation", Journal of Structural Engineering, 122(8), pp. 972–976, 1996. https://doi.org/10.1061/(ASCE)0733-9445(1996)122:8(972)

[7] Tsopelas, P., Constantinou, M. C., Kircher, C. A., Whittaker, A. S. "Evaluation of simplified methods of analysis for yielding structures", University of Buffalo (SUNY), Buffalo, NY, USA, Rep. NCEER-97-0012, 1997.

[8] Ramirez, O. M., Constantinou, M. C., Gomez, J. D., Whittaker, A. S. "Evaluation of simplified methods of analysis of yielding structures with damping systems", Earthquake Spectra, 18(3), pp. 501–530, 2002. https://doi.org/10.1193/1.1509763

[9] Pavlou, E. A., Constantinou, M. C. "Response of elastic and inelastic structures with damping systems to near-field and soft-soil ground motions", Engineering Structures, 26(9), pp. 1217–1230, 2004. https://doi.org/10.1016/j.engstruct.2004.04.001

[10] Fadi, F., Constantinou, M. C. "Evaluation of simplified methods of analysis for structures with triple friction pendulum isolators", Earthquake Engineering Structural Dynamics, 39(1), pp. 5–22, 2010. https://doi.org/10.1002/eqe.930

[11] Ozdemir, G., Constantinou, M. C. "Evaluation of equivalent lateral force procedure in estimating seismic isolator displacements", Soil Dynamics and Earthquake Engineering, 30, pp. 1036–1042, 2010. https://doi.org/10.1016/j.soildyn.2010.04.015

[12] Dao, N. D., Nguyen-Van, H., Nguyen, T. H. A., Chung, A. B. "A new statistical equation for predicting nonlinear time history displacement of seismic isolation systems", Structures, 24, pp. 177–190, 2020.
https://doi.org/10.1016/j.istruc.2020.01.019

[13] Chopra, A. K., Goel, R. K. "Evaluation of NSP to Estimate Seismic Deformation: SDF Systems", Journal of Structural Engineering, 126(4), pp. 482–490, 2000.
https://doi.org/10.1061/(ASCE)0733-9445(2000)126:4(482)

[14] Franchin, P., Monti, G., Pinto, P. E. "On the accuracy of simplified methods for the analysis of isolated bridges", Earthquake Engineering Structural Dynamics, 30(3), pp. 363–382, 2001.
https://doi.org/10.1002/eqe.12

[15] Miranda, E., Ruiz-Garcia, J. "Evaluation of approximate methods to estimate maximum inelastic displacement demands", Earthquake Engineering Structural Dynamics, 31(3), pp. 539–560, 2002.
https://doi.org/10.1002/eqe.143

[16] Warn, G. P., Whittaker, A. S. "Performance estimates in seismically isolated bridge structures", Engineering Structures, 26(9), pp. 1261–1278, 2004.
https://doi.org/10.1016/j.engstruct.2004.04.006

[17] Ryan, K. L., Chopra, A. K. "Estimating the seismic displacement of friction pendulum isolators based on non-linear response history analysis", Earthquake Engineering Structural Dynamics, 33(3), pp. 359–373, 2004.
https://doi.org/10.1002/eqe.355

[18] Dwairi, H. M., Kowalsky, M. J., Nau, J. M. "Equivalent damping in support of direct displacement-based design", Journal of Earthquake Engineering, 11(4), pp. 512–530, 2007.
https://doi.org/10.1080/13632460601033884

[19] Naeim, F., Kelly, J. M. "Design of Seismic Isolated Structures: From Theory to Practice", John Wiley and Sons, NY, USA, 1999.

[20] Kelly, T. E. "Base Isolation of Structures: Design Guidelines", Holmes Consulting Group Ltd., Auckland, New Zealand, 2001.

[21] Erduran, E., Dao, N. D., Ryan, K. L. "Comparative response assessment of minimally compliant low-rise conventional and base-isolated steel frames", Earthquake Engineering Structural Dynamics, 40(10), pp. 1123–1141, 2011.
https://doi.org/10.1002/eqe.1078

[22] Pant, D. R., Constantinou, M. C., Wijeyewickrema, A. C. "Re-evaluation of equivalent lateral force procedure for prediction of displacement demand in seismically isolated structures", Engineering Structures, 52, pp. 455–465, 2013.
https://doi.org/10.1016/j.engstruct.2013.03.013

[23] Chopra, A. K. "Dynamics of structures: theory and applications to earthquake engineering", Prentice Hall, Upper Saddle River, NJ, USA, 2015

[24] Park, J.-G., Otsuka, H. "Optimal yield level of bilinear seismic isolation devices", Earthquake Engineering Structural Dynamics, 28(9), pp. 941–955, 1999.
https://doi.org/10.1002/(SICI)1096-9845(199909)28:9<941::AID-EQE848>3.0.CO;2-5

[25] Mavronicola, E, Komodromos, P "Assessing the suitability of equivalent linear elastic analysis of seismically isolated multi-storey buildings", Computers & Structures, 89(21–22), pp. 1920–1931, 2011.
https://doi.org/10.1016/j.compstruc.2011.05.010

[26] Liu, T., Zordan, T., Briseghella, B., Zhang, Q. "Evaluation of equivalent linearization analysis methods for seismically isolated buildings characterized by SDOF systems", Engineering Structures, 59(2), pp. 619–634, 2014.
https://doi.org/10.1016/j.engstruct.2013.11.028

[27] DIS "Seismic isolation for buildings and bridges", Dynamic Isolation Systems, Reno, NV, USA, 2007.

[28] Pan, P., Zamfirescu, D., Nakashima, M., Nakayasu, N., Kashiwa, H. "Base-isolation design practice in Japan: Introduction to the Post-Kobe approach", Journal of Earthquake Engineering, 9(1), pp. 147–171, 2005.
https://doi.org/10.1080/13632460509350537

[29] Virtanen, P., Gommers, R., Oliphant, T. E., Haberland, M., Reddy, T., …, SciPy 1.0 Contributors "SciPy 1.0: fundamental algorithms for scientific computing in Python", Nature Methods, 17(3), pp. 261–272, 2020.
https://doi.org/10.1038/s41592-019-0686-2